

Guanidine-Containing Molecular Transporters: Sorbitol-Based Transporters Show High Intracellular Selectivity toward Mitochondria**

Kaustabh K. Maiti, Woo Sirl Lee, Toshihide Takeuchi, Catherine Watkins, Marjan Fretz, Dong-Chan Kim, Shiroh Futaki, Arwyn Jones, Kyong-Tai Kim, and Sung-Kee Chung*

The therapeutic efficacy of a drug depends on its ability to reach the desired target tissues, cells, and even intracellular organelles. However, these biological structures are highly protected by various membranes that have evolved in such a way that only a very limited number of foreign molecules are allowed to enter them. The biological barriers include, for example, cellular plasma membranes, the blood–brain barrier (BBB), and nuclear and mitochondrial membranes. It is generally known that the plasma membrane allows entrance only to those molecules with an appropriate range of molecular size, polarity, and charge. Hence, many drug candidates with promising in vitro activities fail to be developed into useful pharmaceutical agents.

The production of molecular transporters to overcome these biological barriers would be highly desirable in drug development. In this context, a number of cell-penetrating peptides (CPPs) derived from HIV-1 Tat protein, Antenna-

pedia protein of *Drosophila*, and related peptides^[1–4] have been extensively studied to improve the absorption, distribution, metabolism, and elimination (ADME) properties of poorly bioavailable drugs including small molecules,^[5] proteins,^[6,7] nucleic acids, and genes.^[8,9] However, the peptide-based molecular transporters are susceptible to a variety of endogenous proteases in the body, thus limiting their bioavailability.

More recently, several research groups have developed synthetic molecular transporters based on peptoids,^[10] oligo-carbamates,^[11] β -peptides,^[12,13] peptide nucleic acids,^[14] and others.^[15–17] We also have recently reported a novel class of guanidine-containing molecular transporters based on inositol dimers as the scaffold. These structures were synthesized by connecting two units of *myo*- or *scyllo*-inositol through a carbonate or amide linkage, and multiple units of the guanidine functionality were elaborated onto these scaffolds by peracylation with an ω -aminocarboxylate derivative of varying chain lengths.

These transporters exhibited very high membrane-translocating properties in simian kidney (COS-7), mouse macrophage (RAW264.7), and HeLa cells, and they were distributed largely in cytosol. Their internalization mechanism, although unclear, and localization patterns appeared to be quite different from those observed with arginine-rich transporters. Furthermore, in the in vivo mouse model studies some of them were found to cross the BBB efficiently and show preferential distributions in heart, lung, and brain over liver, kidney, and spleen.^[18,19] These results have strongly suggested to us that achieving intracellular and/or tissue selectivity might be possible by varying the structural components in the molecular transporter design, such as scaffold, linker chain, and number of guanidine residues, with concomitant modifications of physicochemical properties. Herein, we report molecular transporters that exhibit high selectivity for mitochondrial localization and also overcome the BBB.

Although the previously reported G8 molecular transporters based on dimeric inositol scaffolds showed some interesting and useful properties, such as BBB penetration, we decided to change the scaffold and the linking pattern while staying with eight units of the guanidine residue. Thus, we have designed a series of molecular transporters based on the sorbitol scaffold and bifurcated linkers each carrying two residues of guanidine. Sorbitol (D-glucitol) occurs widely in plants, especially in the *Rosaceae* family, which includes apples, pears, cherries, and apricots. Sorbitol is commercially

[*] Dr. K. K. Maiti, W. S. Lee, Prof. Dr. S.-K. Chung
Department of Chemistry
Pohang University of Science and Technology
Pohang 790-784 (Korea)
Fax: (+82) 54-279-3399
E-mail: skchung@postech.ac.kr
Homepage: <http://www.postech.ac.kr/chem/skc-lab>

T. Takeuchi, Prof. Dr. S. Futaki
Institute for Chemical Research
Kyoto University
Uji, Kyoto 611-0011 (Japan)
and
SORST, Japan Science and Technology Corporation (JST)
Kawaguchi, Saitama 332-0012 (Japan)

D.-C. Kim, Prof. Dr. K.-T. Kim
Department of Life Science
Pohang University of Science and Technology
Pohang 790-784 (Korea)

C. Watkins, M. Fretz, Prof. Dr. A. Jones
Welsh School of Pharmacy
Cardiff University
Cardiff CF103XF (UK)

[**] We thank Sun-Hee Lee for technical assistance involving cell culture and CLSM operation at Postech. Financial support from BK-21 and MOST (National Frontier Research Program administered through KRICT/CBM), and Grants-in-Aid for Scientific Research from the Ministry of Education, Culture, Sports, Science, and Technology of Japan are gratefully acknowledged. T.T. is grateful for a JSPS research fellowship for young scientists. Part of this work (A.J., C.W.) was supported by BBSRC.

Supporting information for this article is available on the WWW under <http://www.angewandte.org> or from the author.

produced by reducing D-glucose or D-glucono-1,4-lactone, and is extensively used in the food industry, as it is highly water soluble and free of any discernible toxicity.^[20]

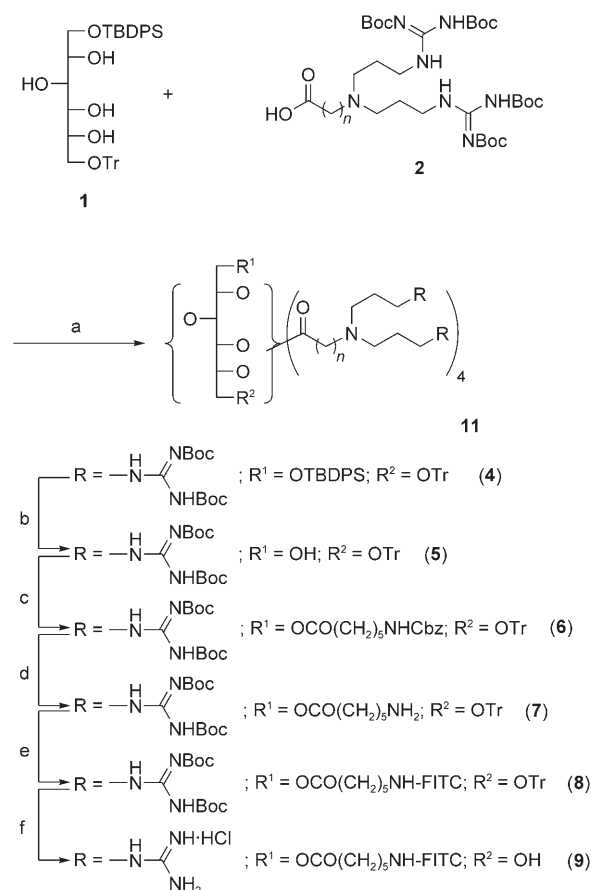
6-*O*-Trityl- α -D-glucose, prepared from α -D-glucose according to the literature procedure,^[21,22] was reduced with NaBH₄ in methanol to produce 6-*O*-trityl-D-sorbitol. The primary hydroxy group in the tritylated sorbitol was selectively protected with *tert*-butyldiphenylsilyl chloride (TBDPS-Cl) and triethylamine (TEA) in pyridine to afford 1-*O*-(*tert*-butyldiphenylsilyl)-6-*O*-trityl-D-sorbitol (**1**, see Scheme 1) in good yield (see Scheme 1 in the Supporting Information for details).

Two types of branched chain containing the bisguanidine moiety were prepared. In the first type, a double Michael addition of ω -aminocarboxylate (with varying chain length, $n = 5$ and 7) to a large excess of acrylonitrile in glacial acetic acid afforded the dicyanoethylated ω -aminocarboxylate products in good yields.^[23,24] The cyano functionality was quantitatively converted to the corresponding amino group by catalytic hydrogenation over Raney Ni in 1N NaOH. The guanidinylation of these intermediates with *N,N'*-di-Boc-*N''*-trifluoromethanesulfonylguanidine and TEA in 1,4-dioxane/water (5:1) provided the requisite bisguanidinylated carboxylic acids **2a** and **2b** (see Scheme 1) in reasonable yields (68 and 74 %).

For construction of the second type of branched chain, the polyamidoamine dendrimer-type process was employed. Thus, the Michael addition between methyl acrylate and 6-aminocaproic acid, followed by exhaustive amidation of the resulting diester with an excess amount of ethylenediamine, gave the bisaminocarboxylate after thorough removal of ethylenediamine by co-evaporation with toluene. The guanidinylation of the amino groups as previously described gave the bisguanidinylated carboxylic acid **3** (see Scheme 2) in 68 % yield after column chromatography (see Scheme 2 of the Supporting Information for details).

The exhaustive acylation of the scaffold, 1-*O*-(*tert*-butyldiphenylsilyl)-6-*O*-trityl-D-sorbitol (**1**), with bisguanidinylated carboxylic acids **2a** and **2b** in dry CH₂Cl₂ in the presence of EDC and DMAP gave compounds **4a** and **4b** in good yields after column chromatography on silica gel (Scheme 1). Selective removal of the TBDPS group in **4** with TBAF in dry THF, to give **5**, was followed by the introduction of a new amino functionality on that hydroxy group. Thus, acylation of **5** with Cbz-protected aminocaproic acid under the EDC coupling conditions furnished the desired products **6** after the usual workup and purification. After deprotection of the *N*-Cbz group in **6** to give **7**, a fluorescence probe was attached by reaction with fluorescein-5-isothiocyanate (FITC) to afford the FITC-labeled compounds **8** in approximately 70 % yield after purification by flash column chromatography. The target molecular transporters **9a** and **9b** were obtained as HCl salts by deprotecting the Boc groups on the guanidine moieties with ethyl acetate saturated with gaseous HCl, and purification by medium-pressure liquid chromatography (MPLC) on a reversed-phase (C8) column (Scheme 1).

Next, we introduced the alternative linker **3** into the sorbitol scaffold **1** by exhaustive acylation under the EDC

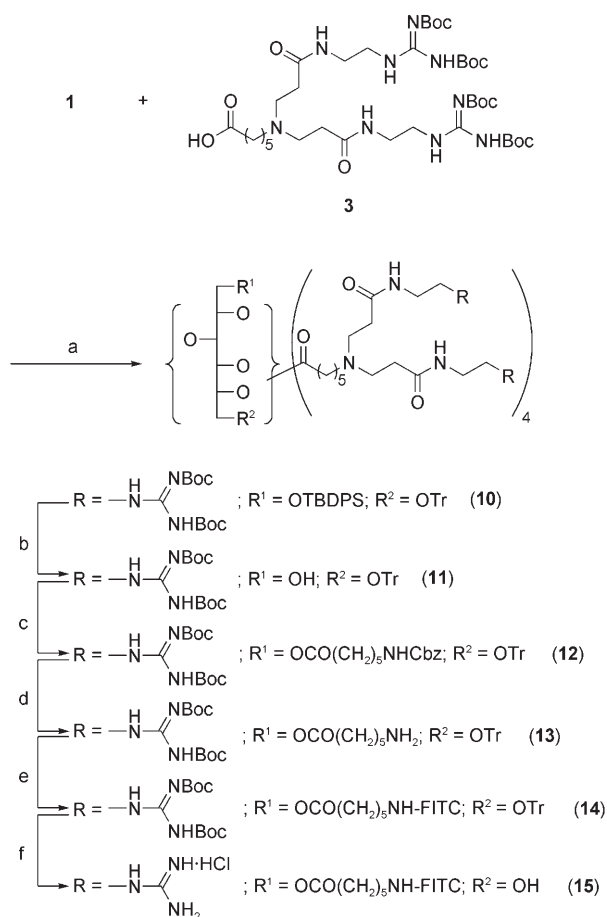


Scheme 1. Synthesis of transporters **9**; **a**: $n = 5$; **b**: $n = 7$. Reagents and conditions: **a**) **2**, EDC, DMAP, CH₂Cl₂, RT, 30 h (**4a**, 66%; **4b**, 92%); **b**) TBAF, THF, RT, 10 h (**5a**, 79%; **5b**, 68%); **c**) *N*-Cbz-protected aminocaproic acid, EDC, DMAP, CH₂Cl₂, RT, 10 h (**6a**, 71%; **6b**, 74%); **d**) 10% Pd/C (10 mol%), H₂ (1 atm), MeOH, RT, 25 h (**7a**, 91%; **7b**, 87%); **e**) FITC (isomer I), TEA, absolute EtOH/THF (5:2), RT, dark, 24 h (**8a**, 68%; **8b**, 61%); **f**) HCl(g), EtOAc, RT, 20 h (**9a**, 81%; **9b**, 86%). EDC = 3-(3-dimethylaminopropyl)-1-ethylcarbodiimide; DMAP = 4-(dimethylamino)pyridine; TBAF = tetrabutylammonium fluoride; Cbz = benzyloxycarbonyl; Boc = *tert*-butoxycarbonyl.

conditions to obtain **10** (Scheme 2), which was then transformed to another type of molecular transporter **15** by procedures analogous to those described for compounds **9**. All key intermediates and the final target compounds **9a**, **9b**, and **15** were thoroughly characterized by HPLC, NMR spectroscopy, and MALDI-TOF mass spectrometry.

Preliminary evaluations of the synthetic transporters for their uptake ability in HeLa cells were carried out by confocal laser scanning microscopy (CLSM). Even after incubation for 15 min at 37 °C with 10 μ M of transporters, cells were substantially marked by fluorescence. The cells were analyzed without fixing and the extents of cellular uptake were visually compared with FITC-labeled arginine nonamer (**R9-FI**) as the reference. A significant fluorescence signal was observed for **9a**, **9b**, and **R9-FI**, but internalization of **15** appeared to be much less than with the others.

More detailed fluorescence-activated cell-sorter (FACS) studies were carried out in terms of the concentration and



Scheme 2. Synthesis of transporter **15**. Reagents and conditions: a) **3**, EDC, DMAP, CH_2Cl_2 , RT, 30 h, 62%; b) TBAF, THF, RT, 15 h, 80%; c) *N*-Cbz-protected aminocaproic acid, EDC, DMAP, CH_2Cl_2 , RT, 18 h, 72%; d) 10% Pd/C (10 mol%), H_2 (1 atm), MeOH, RT, 20 h, 87%; e) FITC (isomer I) (1.2 equiv), TEA, absolute EtOH/THF (5:2), RT, dark, 24 h, 65%; f) HCl(g), EtOAc, RT, 24 h, 83%.

time dependency (Figure 1A and B). The R8 peptide is known as a representative peptide among the transporters that show highly efficient internalization.^[2] Analyzed by the relative fluorescence intensities, **9a** and **9b** (at 10 μM) had an efficiency almost comparable to that of FITC-labeled R8 (FITC-R8; 10 μM ; Figure 1A). On the other hand, the internalization efficiency of **15** was not nearly as high. In addition, a substantial increase of cellular uptake of **9a** and **9b** was observed when the concentration was raised to 20 μM . Figure 1B shows the kinetics of cellular uptake of these transporters. The cellular uptake almost reaches a plateau in approximately 3 h with **9b** again showing the highest efficiency.

Confocal microscopic observation of the cells treated with these transporters demonstrated that **9a** and **9b** yielded very similar cytoplasmic distributions (Figure 2A). Transporter **15** gave only very faint fluorescence signals in the same experiment. As it seemed likely that **9a** and **9b** co-localized with some vesicular components with very similar cytoplasmic localization, we selected **9a** for a more detailed study of cytoplasmic localization of the vectors. Internalization of **9a**

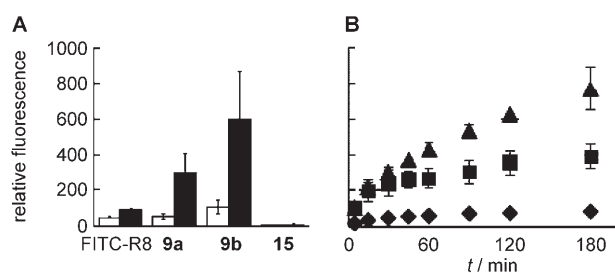


Figure 1. Cellular uptake of sorbitol-based transporters. A) FACS quantification of the transporters taken up by HeLa cells. Cells were treated with transporters **9a**, **9b**, **15**, and FITC-labeled R8 peptide in serum-containing medium at 37°C for 1 h and then analyzed by FACS. Open and filled columns represent the uptake by the cells treated with 10 and 20 μM transporters, respectively. B) Kinetics in cellular uptake of transporters. HeLa cells were incubated with **9a** (\blacksquare), **9b** (\blacktriangle), and **15** (\blacklozenge) (10 μM each) at 37°C for the time indicated and analyzed by FACS. Data shown means with \pm standard deviation from three samples.

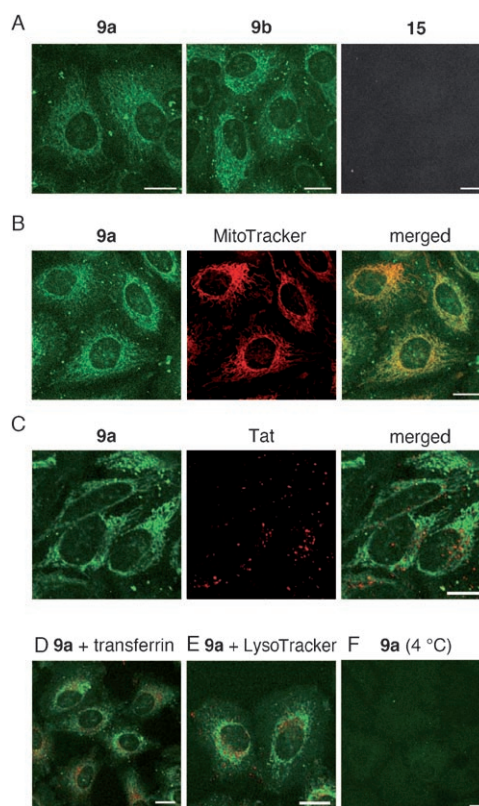


Figure 2. Cellular localization of sorbitol-based transporters. A) Confocal microscopic observation of HeLa cells treated with **9a**, **9b**, and **15** (10 μM each) at 37°C for 1 h. B) Mitochondrial localization of transporter **9a**. The cells were treated with **9a** (green; 10 μM) and MitoTracker (red; 250 nM) at 37°C for 1 h. No significant co-localization of the signals of **9a** (green) with C) Tat peptide (10 μM), D) transferrin (25 $\mu\text{g mL}^{-1}$) labeled with tetramethylrhodamine, and E) LysoTracker (50 nM, red) was observed after co-incubation at 37°C for 1 h. F) A significant decrease in internalization of **9a** (10 μM) occurred on incubation at 4°C for 1 h. Scale bars: 20 μm .

was significantly inhibited at 4°C (Figure 2F), apparently suggesting an involvement of energy-dependent steps in this internalization. Figure 2C–E clearly shows that 1) there is

little or no co-localization between **9a** and tetramethylrhodamine-labeled Tat peptide or transferrin, which strongly suggests a different uptake mechanism for **9a** from those of Tat peptide and transferrin, and 2) a major portion of **9a** did not reach lysosomes or acidic endosomes stained by LysoTracker in 1 h. However, to our surprise significant co-localization of **9a** and mitochondria-specific dye, MitoTracker Red, was observed (Figure 2B and Figure 1 of the Supporting Information), which suggests accumulation of **9a** in mitochondria after the cellular uptake. Transporter **9b** also showed similar co-localization with MitoTracker in HeLa cells (data not shown). These observations are highly significant, especially as Tat and the related peptides do not show significant mitochondrial localization.^[25]

Molecular transporters capable of selectively delivering a drug or cargo to mitochondria are desperately needed in the diagnosis and treatment of mitochondrial diseases.^[26] A heterocyclic tetraguanidinium compound, which has a skeletal frame somewhat reminiscent of those of the heterocyanine dyes and the cyclic iminium structure of MitoTracker Red, was reported to target mitochondria,^[16] but its potential utility might be somewhat limited because the observation was made with fixed cells and it showed significant toxicity even at 10 μM . The novel structure and synthetic ease of transporters **9a** and **9b** may provide a new platform for the design of further mitochondrial-targeting systems.^[27]

Mitochondrial defects are known to occur in a wide variety of degenerative diseases, aging, and even cancer. Abnormal mitochondria have been associated with many diseases including maternally inherited Leber hereditary optic neuropathy (LHON), progressive external ophthalmoplegia (PEO), Kearns–Sayre Syndrome (KSS), mitochondrial encephalomyopathy, lactic acidosis and stroke-like syndrome (MELAS), myoclonic epilepsy and ragged-red fibers (MERRF), and a cluster of metabolic diseases (syndrome X).^[28] In addition, mitochondria are known to play key roles in apoptosis (cancer therapy),^[29] familial amyotrophic lateral sclerosis (ALS, Lou Gehrig’s disease),^[30] Huntington’s disease,^[31] and Alzheimer’s disease.^[32]

In view of the significant observation that these transporters efficiently migrate to mitochondria in HeLa cells, the cellular distribution of compound **9b** was also analyzed in CD34⁺ stem-cell-like KG1a leukemia cells, which had previously been characterized with respect to interactions with CPPs.^[33,34] KG1a cells incubated with compound **9b** for 1 h at 37 $^{\circ}\text{C}$ are clearly labeled but there is some heterogeneity with respect to the degree of labeling (see Figure 2 of the Supporting Information).^[35] Co-incubation experiments with **9b** and MitoTracker confirmed our previous analyses in HeLa cells, again showing extensive co-localization. The full extent of co-localization is most apparent when the cells are analyzed through the *xyz* axes.

Although mitochondrial localization sequences (MLSs) and endogenous mitochondrial metabolite transporters have been reported, it is unlikely on a structural basis that the selective targeting of compounds **9a** and **9b** is related to these. Rhodamine 123 and cyanine dyes are the best-known mitochondriotropic compounds, and the structural features required for affinity have been proposed to be amphiphilicity

combined with π -electron density delocalization over more than three atoms (“delocalized cations”).^[26] As the mitochondrial membrane is known to have a high membrane potential with negative charges present on the cytosolic side, it can be readily imagined that the positive charges present on the guanidinium residues of the transporter help its interaction with the mitochondrial membrane. However, it is not clear at this stage what specific structural features (for example, sorbitol scaffold, number of guanidine units, or branched-linker pattern) of the transporters are responsible for the observed organellar selectivity, especially as neither R8 nor the dimeric inositol-based transporters show this selectivity.^[18,25] However, in two very different cell lines there is clear sequestration of these compounds in mitochondria, which suggests that they may be useful vectors for mitochondrial delivery.

Next, we examined the tissue-distribution patterns of compound **9a** in mice (Figure 3). Transporter **9a** (HCl salt, 82 mg kg^{-1}) was dissolved in sterile distilled water and

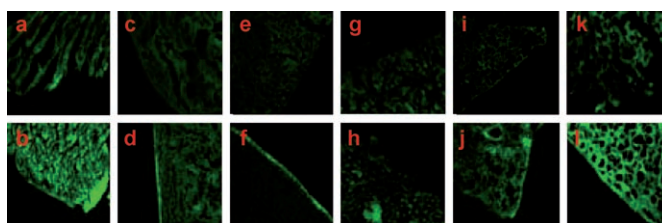


Figure 3. Distribution of **9a** (HCl salt) in mouse tissue (bottom; top: control). Fluorescence micrographs of heart muscle (a, b), spleen (c, d), liver (e, f), kidney (g, h), and lung (i, j) tissue sections, and of coronal brain sections (k, l) isolated from mice 20 min after i.p. injection. Exposure time [ms]: 14 000 (a, b); 500 (c, d); 300 (e, f); 500 (g, h); 1200 (i, j); 15 000 (k, l); $\lambda_{\text{max}} = 488 \text{ nm}$ (green fluorescence from FITC).

injected intraperitoneally (i.p.) into 8-week-old mice (C57BL/6). After 20 min, the treated mice were perfused with 4% paraformaldehyde in phosphate buffer solution (PBS; pH 7.4), and the organs including the heart, spleen, liver, kidneys, lungs, and brain were incubated overnight in a solution of 0.5M sucrose in PBS. Placed in cryoprotectant, they were cut into 15- μm sections with a cryostat and transferred to coated glass slides. After drying at 37 $^{\circ}\text{C}$, the sections were washed with PBS and treated with 0.3% Triton X-100 for 15 min at room temperature, and analyzed with an Axioplan2 fluorescence imaging microscope (Carl Zeiss).

The Tat peptides were previously reported to show wide distributions in the liver, kidneys, lungs, heart muscle, and spleen,^[36,37] and the synthetic transporters based on the dimeric inositol scaffold were shown to be distributed predominantly in the heart, lung, and brain tissues.^[18] With transporter **9a**, a higher distribution was found in the heart muscle and brain sections than in any other tissue examined. It might be possible that the observed tissue selectivity is related to the organellar selectivity of **9a** toward mitochondria, as the heart and brain are presumably quite active in energy metabolism. An alternative possibility might be that

there is some specific interaction between the transporter and a cell-surface component of brain and heart tissues.

In summary, in the hope of achieving some intracellular organellar and/or in vivo tissue selectivity, we have designed and synthesized transporter molecules based on the sorbitol scaffold, which is structurally elaborated to carry eight residues of guanidine base through two different types of branched chains. One type (**9a** and **9b**) of these transporters is shown to be efficiently cell-penetrating, and to possess unique intracellular selectivity toward mitochondria as well as some interesting tissue selectivity for heart and brain in mice. At the moment, it is not clear which structural features or physicochemical properties of these transporters contribute to the observed selectivity. We speculate that the mitochondrial affinity and the preferential distribution in heart and brain might be related, with potential implications in the practical delivery of drugs in the therapy of cancers and diseases related to the central nervous system. Further studies aimed at elucidating the structure–selectivity relationship of these guanidine-containing transporters and exploring their applications are ongoing.

Received: March 28, 2007

Published online: July 2, 2007

Keywords: bioorganic chemistry · carbohydrates · drug delivery · membranes · mitochondria

- [1] *Handbook of Cell-Penetrating Peptides*, 2nd ed. (Ed.: Ü. Langel), CRC, Boca Raton, **2006**.
- [2] S. Futaki, *Adv. Drug Delivery Rev.* **2005**, *57*, 547.
- [3] S. Futaki, T. Suzuki, W. Ohashi, T. Yagami, S. Tanaka, K. Ueda, Y. Sugiura, *J. Biol. Chem.* **2001**, *276*, 5836.
- [4] A. Joliot, A. Prochiantz, *Nat. Cell Biol.* **2004**, *6*, 189.
- [5] J. B. Rothbard, S. Garlington, O. Lin, T. Kirschberg, E. Kreider, P. L. McGrane, P. A. Wender, P. A. Khavari, *Nat. Med.* **2000**, *6*, 1253.
- [6] J. S. Wadia, R. V. Stan, S. F. Dowdy, *Nat. Med.* **2004**, *10*, 310.
- [7] I. Nakase, M. Niwa, T. Takeuchi, K. Sonomura, N. Kawabata, Y. Koike, M. Takehashi, S. Tanaka, K. Ueda, J. C. Simpson, A. T. Jones, Y. Sugiura, S. Futaki, *Mol. Ther.* **2004**, *10*, 1011.
- [8] V. P. Torchilin, R. Rammohan, V. Weissig, T. S. Levchenko, *Proc. Natl. Acad. Sci. USA* **2001**, *98*, 8786.
- [9] K. Kogure, R. Moriguchi, K. Sasaki, M. Ueno, S. Futaki, H. Harashima, *J. Controlled Release* **2004**, *98*, 317.
- [10] P. A. Wender, D. J. Mitchell, K. Pattabiraman, E. T. Pelkey, L. Steinman, J. B. Rothbard, *Proc. Natl. Acad. Sci. USA* **2000**, *97*, 13003.
- [11] P. A. Wender, J. B. Rothbard, T. C. Jessop, E. L. Kreider, B. L. Wylie, *J. Am. Chem. Soc.* **2002**, *124*, 13382.
- [12] N. Umezawa, M. A. Gelman, M. C. Haigis, R. T. Raines, S. H. Gellman, *J. Am. Chem. Soc.* **2002**, *124*, 368.
- [13] N. Rueping, Y. Mahajan, M. Sauer, D. Seebach, *ChemBioChem* **2002**, *3*, 257.
- [14] P. Zhou, M. Wang, L. Du, G. W. Fisher, A. Waggoner, D. H. Ly, *J. Am. Chem. Soc.* **2003**, *125*, 6878.
- [15] N. W. Luedtke, P. Carmichael, Y. Tor, *J. Am. Chem. Soc.* **2003**, *125*, 12374.
- [16] J. Fernandez-Carneado, M. Van Gool, V. Martos, S. Castel, P. Prados, J. de Mendoza, E. Giralt, *J. Am. Chem. Soc.* **2005**, *127*, 869.
- [17] H. H. Chung, G. Harms, C. M. Seong, B. H. Choi, C. Min, J. P. Taulane, M. Goodman, *Biopolymers* **2004**, *76*, 83.
- [18] K. K. Maiti, O. Y. Jeon, W. S. Lee, D. C. Kim, K. T. Kim, T. Takeuchi, S. Futaki, S. K. Chung, *Angew. Chem.* **2006**, *118*, 2973; *Angew. Chem. Int. Ed.* **2006**, *45*, 2907.
- [19] K. K. Maiti, O. Y. Jeon, W. S. Lee, S. K. Chung, *Chem. Eur. J.* **2007**, *13*, 762.
- [20] J. S. Brimacombe, J. M. Webber in *Carbohydrates: Chemistry and Biochemistry*, Vol. 1, 2nd ed. (Ed.: W. Pigman, D. Horton), Academic Press, New York, **1972**, p. 479.
- [21] S. K. Chaudhary, O. Hernandez, *Tetrahedron Lett.* **1979**, *20*, 95.
- [22] A. Klemer, K. Homberg, *Chem. Ber.* **1961**, *94*, 491.
- [23] F. M. Braña, G. Dominguez, B. Saez, C. Romerdahl, S. Robinson, T. Barlozzari, *Eur. J. Med. Chem.* **2002**, *37*, 541.
- [24] M. Dubber, K. T. Lindhorst, *Org. Lett.* **2001**, *3*, 4019.
- [25] a) M. F. Ross, A. Filipovska, R. A. J. Smith, M. J. Gate, M. P. Murphy, *Biochem. J.* **2004**, *383*, 457; b) M. P. Murphy, R. A. Smith, *Annu. Rev. Pharmacol. Toxicol.* **2007**, *47*, 629.
- [26] V. Weissig, S. M. Cheng, G. G. M. D'Souza, *Mitochondrion* **2004**, *3*, 229.
- [27] The parent structures of the present carriers showed 3-(4,5-dimethylthiazol-2-yl)-2,5-diphenyltetrazolium bromide (MTT) toxicity profiles similar to that of R8, that is, virtually no toxicity at 10 μM .
- [28] D. C. Wallace, *Science* **1999**, *283*, 1482.
- [29] D. R. Green, J. C. Reed, *Science* **1998**, *281*, 1309.
- [30] V. L. Dawson, *Nat. Med.* **2004**, *10*, 905.
- [31] B. I. Bae, S. Igarashi, M. Fujimoro, N. Agrawal, Y. Taya, S. D. Hayward, T. H. Moran, C. A. Ross, S. H. Snyder, A. Sawa, *Neuron* **2005**, *47*, 29.
- [32] M. Manczak, T. S. Anekonda, E. Henson, B. S. Park, J. Quinn, P. M. Reddy, *Hum. Mol. Genet.* **2006**, *15*, 1437.
- [33] S. Al-Taei, N. A. Penning, J. C. Simpson, S. Futaki, T. Takeuchi, I. Nakase, A. T. Jones, *Bioconjugate Chem.* **2006**, *17*, 90.
- [34] M. M. Fretz, N. A. Penning, S. Al-Taei, S. Futaki, T. Takeuchi, I. Nakase, I. G. Storm, A. T. Jones, *Biochem. J.* **2007**, *403*, 335.
- [35] This kind of heterogeneity has been occasionally observed, and may be related to cell cycles of individual cells.
- [36] S. R. Schwarze, A. Ho, A. Vocero-Akbani, S. F. Dowdy, *Science* **1999**, *285*, 1569.
- [37] S. R. Cai, G. Xu, M. Backer-Hapak, M. Ma, S. F. Dowdy, H. L. McLeod, *Eur. J. Pharm. Sci.* **2006**, *27*, 311.